

Scalable quantum computation with cavity QED systems

V. Giovannetti,¹ D. Vitali,¹ P. Tombesi,¹ and A. Ekert²

¹*Dipartimento di Matematica e Fisica, Università di Camerino, INFN, Unità di Camerino, via Madonna delle Carceri 62032, Camerino, Italy*

²*Centre for Quantum Computation, Clarendon Laboratory, Parks Road, Oxford OX1 3PU, United Kingdom*

(Received 28 April 2000; published 15 August 2000)

We propose a scheme for quantum computing using high- Q cavities in which the qubits are represented by single-cavity modes restricted in the space spanned by the two lowest Fock states. We show that single-qubit operations and universal multiple qubit gates can be implemented using atoms sequentially crossing the cavities.

PACS number(s): 03.67.Lx, 42.50.Ar, 32.80.Rm

I. INTRODUCTION

In recent years, numerous physical systems have been proposed as possible candidates for the implementation of a quantum computer. The desirable conditions that have to be satisfied are a reliable and easy way to prepare and detect the quantum states of the qubits, the possibility of engineering highly entangled states, the scalability to a large number of qubits, and a very low decoherence rate [1]. Up until now, experimental implementations have involved linear ion traps [2], liquid-state nuclear-magnetic resonance (NMR) [3], and cavity QED systems [4,5]. In the ion trap case, only the controlled-NOT (CNOT) gate between two internal states and the vibrational level of a single ion has been realized [6], and quantum gates involving two or more ions have not yet been realized experimentally. A promising step in this direction is the very recent generation of an entangled state of four ions, even if only with 57% fidelity [7]. The status of liquid-state NMR quantum computing is still debated [8], but the fact that the signal strength becomes exponentially small with the number of qubits makes it certain that this proposal is not scalable to more than about ten qubits. This explains why the research of new physical implementations of a quantum computer is so active (see [9] and references therein). Here, elaborating on the suggestions of Ref. [10], we propose to use the Fock's states $|0\rangle$ and $|1\rangle$ of a high- Q cavity mode as the two logical states of a qubit. A quantum register of N qubits is therefore a collection of N identical cavities in which the state of an appropriately chosen cavity mode is within the space spanned by the vacuum and the one-photon state. The register transformations are achieved by sending off-resonant two-level atoms through the cavities and making them mutually interactive by means of suitable classical fields. With this respect, the present proposal is similar to that of Refs. [11,12]; the important difference is that, in these papers, the logical qubits are represented by two circular Rydberg levels of the atoms. In our proposal, the role of atoms and cavity modes are exchanged. In this way, the present scheme becomes scalable in principle. In practice, its scalability can be limited by the spontaneous emission from the Rydberg levels or by other technical limitations, but the present proposal has the advantage that the needed technology is essentially already available to realize some proof-of-principle demonstrations of quantum computation with few

qubits. In fact, in the present paper we shall specialize to the case of microwave cavities, for which a high level of quantum state control and engineering has already been experimentally shown [5,13]. This is the reason why in our explicit calculations we shall consider microwave cavities operating in low-order modes with angular frequency ω in the 10–100 GHz range, and Rydberg atoms for which high values of the coupling constant (of the order of 10^5 s^{-1}) are possible. It is clear, however, that in principle, the method can be applied to optical cavities too, in which one can have a miniaturization of the scheme and therefore a faster operation.

Some preliminary results regarding the possibilities offered by the present cavity QED scheme have been shown in [14], where some implementations of the CNOT gate between two cavity modes have been presented. In order to give a clear and exhaustive description, here we shall review the results of [14], which will be extended and generalized in the present paper.

The outline of the paper is as follows. In Sec. II we review the basic properties of the considered cavity QED system. In Sec. III we show how to implement the universal CNOT gate between two cavities, while in Sec. IV we shall discuss a different scheme for the implementation of universal two-qubit gates, using an arrangement based on that adopted in the experiment of Ref. [13]. In Sec. V we show how single-qubit operations can be realized, while Sec. VI is devoted to the implementation of useful many-qubit universal quantum gates, such as the Toffoli gate and the encoding and decoding network for quantum error correction schemes. Section VII is for concluding remarks, while the Appendix shows the explicit implementation of the Deutsch problem [15,16].

II. THE SYSTEM

The interaction of a two-level atom quasis resonant with a high- Q cavity mode is well described by the time-dependent Hamiltonian [17]:

$$\mathcal{H}(t) = \frac{\hbar\omega}{2}[b^\dagger b + bb^\dagger] + \frac{\hbar\omega_{eg}}{2}[|e\rangle\langle e| - |g\rangle\langle g|] + \hbar\Omega(t)[|e\rangle\langle g|b + |g\rangle\langle e|b^\dagger], \quad (2.1)$$

in which b and ω are the annihilation operator and the angular frequency of the cavity mode, respectively; $|e\rangle$ and $|g\rangle$ are the excited and lower circular Rydberg states, and $\hbar\omega_{eg}$ is their energy difference. Finally, $\Omega(t)$ is the atom-field interaction Rabi frequency, which is time dependent because of the atomic motion through the cavity. In particular, for a Fabry-Pérot-type cavity, with a Gaussian transverse beam profile, we can assume the following continuous variation:

$$\Omega(t) = \Omega_0 e^{-(t/\tau)^2}, \quad (2.2)$$

$$|\mathcal{V}_{\pm}^{(n)}(t)\rangle = \frac{(\delta/2 \pm \sqrt{(\delta/2)^2 + \Omega^2(t)(n+1)})|e, n\rangle + \Omega(t)\sqrt{n+1}|g, n+1\rangle}{\sqrt{\delta^2/2 + 2\Omega^2(t)(n+1) \pm \delta\sqrt{(\delta/2)^2 + \Omega^2(t)(n+1)}}} \quad (2.3)$$

with eigenvalues

$$E_{\pm}^{(n)}(t) = \hbar\omega(n+1) \pm \hbar\sqrt{(\delta/2)^2 + \Omega^2(t)(n+1)}, \quad (2.4)$$

where $\delta = \omega_{eg} - \omega$ is the atom-cavity detuning. Figure 1 qualitatively shows the time dependence of the dressed levels of Eq. (2.4) in the case $\delta > 0$. Now, if the atom velocity is slow enough, and the system for $t \ll -\tau$ is prepared in a generic energy eigenstate, then in its time evolution it will adiabatically follow this eigenstate, with negligible transitions toward other states [18]. The exact adiabatic condition can be obtained by writing the Schrödinger equation in the basis of the vectors $|\mathcal{V}_{\pm}^{(n)}(t)\rangle$, and then neglecting terms coupling the dressed states. The resulting condition is

$$\frac{\dot{\Omega}(t) \delta \sqrt{n}}{4[(\delta/2)^2 + \Omega^2(t)n]^{3/2}} \ll 1, \quad (2.5)$$

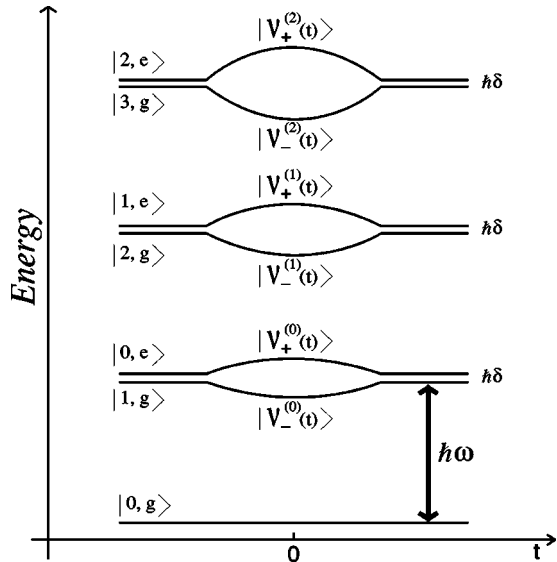


FIG. 1. Energy level of the dressed states as a function of time.

where 2τ is the atomic transit time, which depends of course on the inverse of the atomic velocity. For $|t| \gg \tau$, i.e., when the atom is outside the cavity, the energy eigenvectors of the system are $|g\rangle \otimes |n\rangle \equiv |g, n\rangle$, and $|e, n\rangle$, with $|n\rangle$ as the generic Fock state of the cavity mode. Apart from the ground state $|g, 0\rangle$, which remains unchanged in the presence of the time-dependent interaction, these terms are coupled by photon emission or absorption, and the instantaneous energy eigenstates at fixed time t are the dressed states

which, in the limit $\Omega(t)\sqrt{n}/\delta \ll 1$, becomes equal to that given in Ref. [17]. The general adiabatic condition (2.5) shows in particular that adiabaticity can be obtained even when $\Omega(t)\sqrt{n}/\delta \approx 1$, provided that $\dot{\Omega}(t)$ is sufficiently small. In the following we shall always work in this adiabatic regime.

III. THE CNOT GATE

Domokos *et al.* have shown in Ref. [12] that, using induced transitions between the dressed states, it is possible to implement a CNOT gate in which a cavity containing at most one photon is the control qubit and the atom is the target qubit. This idea is the starting point for the implementation of the CNOT gate between two cavities we propose here. Reference [12] considers an atom adiabatically entering the cavity so that the joint atom-cavity state is

$$c_1|g, 0\rangle + c_2|g, 1\rangle + c_3|e, 0\rangle + c_4|e, 1\rangle. \quad (3.1)$$

When the atom is just inside the cavity, a classical field S of frequency ω_S equal to the energy difference between the dressed states $|\mathcal{V}_+^{(1)}(t=0)\rangle$ (originating from $|e, 1\rangle$) and $|\mathcal{V}_-^{(0)}(t=0)\rangle$ (originating from $|g, 1\rangle$) is switched on for a time interval $2\tau_S$, so that the following driving Hamiltonian is added to $\mathcal{H}(t)$ of Eq. (2.1):

$$\mathcal{H}_S(t) = -\hbar\Xi_0 \cos(\omega_S t + \varphi_S) e^{-(t/\tau_S)^2} [|e\rangle\langle g| + |g\rangle\langle e|], \quad (3.2)$$

where φ_S is the phase of the classical field S and Ξ_0 is the coupling constant, which depends on the dipole moment of the transition $e \leftrightarrow g$ and on the intensity of S . Appropriately choosing the value of τ_S , it is now possible to selectively couple S with these dressed states, leaving the other components of the vector state essentially unperturbed. Moreover, with a suitable choice of the intensity S , it is possible to apply a Rabi π pulse between the two states. In this way, when the atom exits the cavity, the resulting state vector in the interaction picture, apart for some phase terms, is given

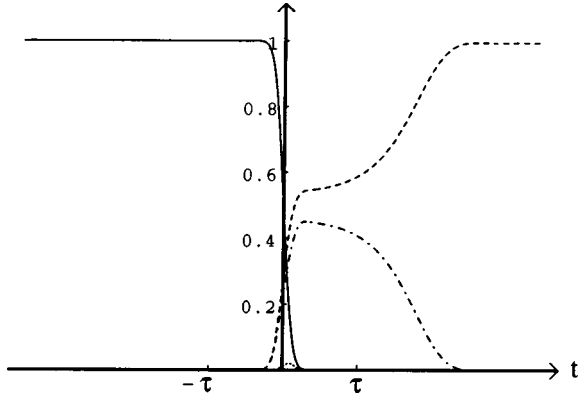


FIG. 2. Time evolution of the population of the dressed states $|g,0\rangle$ (full line), $|\mathcal{V}_-^{(0)}(t)\rangle$ (dashed line), $|\mathcal{V}_+^{(0)}(t)\rangle$ (dotted-dashed line) and $|\mathcal{V}_+^{(1)}(t)\rangle$ (dotted line) for the CNOT(atom \rightarrow cavity) gate with $\Omega_0=420$ kHz, $\delta=0.18\Omega_0$, $\tau\sim 100$ μ s, $\Xi_0=141.5$ kHz, $\tau_S=19$ μ s, and initial condition $|\psi_0\rangle=|g,0\rangle$.

by Eq. (3.1), but with $|e,1\rangle$ and $|g,1\rangle$ exchanged. In this way one has realized a CNOT gate in which, when the cavity (the control qubit) has one photon, the atom undergoes a NOT operation, while when the cavity contains no photons, the atomic state remains unchanged. We shall refer to this gate as the CNOT(cavity \rightarrow atom).

In a similar manner, we can also build a CNOT gate in which the roles of the atom and the cavity are exchanged. Let us in fact tune the frequency ω_S to the transition between the dressed state $|\mathcal{V}_-^{(0)}(t=0)\rangle$ and the state $|g,0\rangle$, and apply again a π pulse inside the cavity as before. Now, when the atom leaves the cavity, the terms $|g,0\rangle$ and $|g,1\rangle$ in the vector state of the system are mutually exchanged with respect to the initial condition Eq. (3.1). The $|e,0\rangle$ and $|e,1\rangle$ components are instead not affected by the interaction with the classical source S . This means having realized a CNOT gate in which, when the atom is in the ground state, the cavity states $|0\rangle$ and $|1\rangle$ flip, while nothing happens to the cavity state for the atom in the excited state. In analogy with the previous case, we refer to this new gate as CNOT(atom \rightarrow cavity).

It is important to note that, differently from the CNOT(cavity \rightarrow atom) case, in the CNOT(atom \rightarrow cavity) gate the Rabi transition between the original states (i.e., $|g,0\rangle$ and $|g,1\rangle$) of the dressed states involved is forbidden by selection rules.

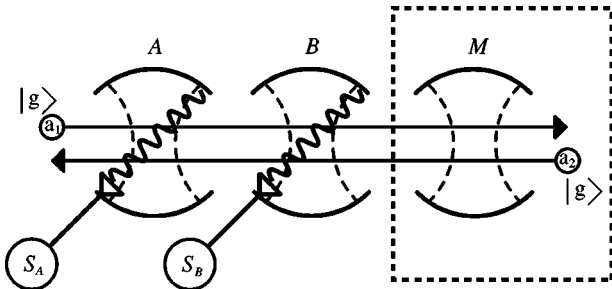


FIG. 3. Schematic description of the CNOT gate in which cavity A is the control qubit and cavity B the target qubit. a_1 and a_2 are the two atoms, and M is the auxiliary cavity, transferring the entanglement with the cavities from the first to the second atom.

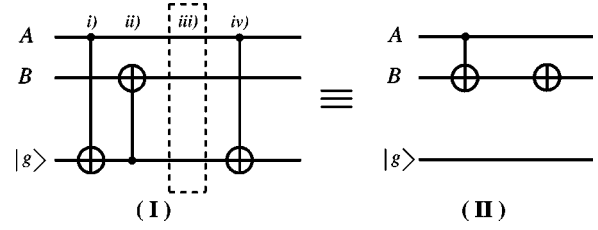


FIG. 4. Logical scheme of the CNOTINV gate of Fig. 3. The dashed box denotes the ‘‘atomic mirror’’ (see Sec. III).

Nevertheless, this coupling is realizable when the atom is in the cavity because the vector $|\mathcal{V}_-^{(0)}(t=0)\rangle$ also has a $|e,0\rangle$ component. However, since this dependence is mediated by a coefficient that decreases with Ω_0/δ [see Eq. (2.3)], we have to choose a value of this parameter that is not too small in order to have a significant coupling constant. In particular, in our calculations we have chosen $\Omega_0/\delta\sim 10^{-1}$. With such values for δ , it is also possible to have a sufficient frequency separation between the transitions we are interested in and all the other ones. Actually, it is sufficient to set the duration of the classical pulse $2\tau_S$ of the order of 20 μ s to discriminate all the parasitic transitions and optimal results for the resulting quantum operation that are achieved for $\Omega_0=420$ kHz, $\delta=0.18\Omega_0$, $\tau\sim 100$ μ s and with $\Xi_0=240$ kHz, $\tau_S=14$ μ s for the CNOT(cavity \rightarrow atom), $\Xi_0=141.5$ kHz, $\tau_S=19$ μ s for the CNOT(atom \rightarrow cavity). In Fig. 2 we show the time evolution of the dressed state populations for the CNOT(atom \rightarrow cavity) for the above choice of parameter values.

For quantum information processing, one needs to control not only the level populations, but also the relative phases. In general, during the adiabatic evolution, different dynamical phases for the different components of the vector state are generated. However, it is always possible to correct these phases by an appropriate choice of the field phase φ_S and by eventually acting outside the cavity on the atom with suitable Stark electric fields.

We now have all the elements to realize the CNOT gate between two distinct but identical cavities A and B , with the first one acting as the control qubit and the second one as the target qubit. The apparatus is sketched in Fig. 3 and it is essentially a physical realization of the logical network shown in Fig. 4. Suppose that the initial states of the two cavities are, respectively, $|\phi\rangle_A=\alpha_A|0\rangle_A+\beta_A|1\rangle_A$ and $|\psi\rangle_B=\alpha_B|0\rangle_B+\beta_B|1\rangle_B$. The following occurs: (i) A first atom, a_1 , prepared in the ground state $|g\rangle$, enters cavity A , where it undergoes the CNOT(cavity \rightarrow atom) transformation realized with the classical field source S_A , and described above.

(ii) Then a_1 leaves A and enters cavity B : here the classical field S_B is switched on in order to obtain a CNOT(atom \rightarrow cavity) transformation. In the interaction picture and neglecting all the parasitic but controllable phase terms, the state of the total system at this stage is then

$$\alpha_A|0\rangle_A\otimes\overline{|\psi\rangle}_B\otimes|g\rangle+\beta_A|1\rangle_A\otimes|\psi\rangle_B\otimes|e\rangle, \quad (3.3)$$

where $\overline{|\psi\rangle}_B$ is the NOT-conjugate vector of $|\psi\rangle_B$, that is, $\beta_B|0\rangle_B+\alpha_B|1\rangle_B$.

(iii) and (iv) The atom again enters A , where it undergoes the CNOT(cavity \rightarrow atom) transformation, so that the state of the system becomes

$$\begin{aligned} & \alpha_A |0\rangle_A \otimes \overline{|\psi\rangle}_B \otimes |g\rangle + \beta_A |1\rangle_A \otimes |\psi\rangle_B \otimes |g\rangle \\ & = \{\alpha_A |0\rangle_A \otimes \overline{|\psi\rangle}_B + \beta_A |1\rangle_A \otimes |\psi\rangle_B\} \otimes |g\rangle. \end{aligned} \quad (3.4)$$

In terms of the notations given in the preceding section, we shall refer to this gate as the CNOTINV($A \rightarrow B$) gate, in order to underline that B transforms to a NOT transformation when A is in the $|0\rangle_A$ state, while nothing happens when A is in the $|1\rangle_A$ state. This fact is illustrated in Fig. 4, where in the equivalent gate **(II)** there is a NOT transformation acting on B .

The practical realization of step (iii), i.e., the return of the atom in the first cavity, is actually more complicated than what it looks like in Figs. 3 and 4. The inversion of the motion of atom a_1 could be realized in principle with an atomic fountain configuration. However, this implies having free-fall velocities, which are too slow for the necessary interaction times to occur within the cavities. For this reason we propose transferring the quantum information from this atom onto a second one of the same type, but traveling in the opposite direction. With this respect, the scheme adopts the ‘‘quantum memory’’ scheme experimentally verified in Ref. [19]. This quantum information transfer is implemented by introducing a third cavity, the auxiliary cavity M of Fig. 3, which, differently from A and B , is resonant with the $e \rightarrow g$ transition. If M is prepared in the vacuum state $|0\rangle_M$, and the transit time of a_1 is appropriately chosen, then the atomic state component $|e\rangle$ releases one photon in M through a resonant π Rabi oscillation. After that, the state of the total system (the three cavities and a_1), using the same notations of Eq. (3.3), will be

$$\alpha_A |0\rangle_A \otimes \overline{|\psi\rangle}_B \otimes |g\rangle \otimes |0\rangle_M + \beta_A |1\rangle_A \otimes |\psi\rangle_B \otimes |g\rangle \otimes |1\rangle_M. \quad (3.5)$$

Notice that the entanglement of a_1 with A and B is now transferred to the auxiliary cavity M : the state of the atom a_1 is factorized and it can be neglected from now on. At this stage, a second atom a_2 is prepared in the ground state $|g\rangle$ and injected into the apparatus with the same absolute value of the velocity of a_1 , but with the opposite direction. Entering M , it absorbs the photon left by the first atom through a similar π Rabi oscillation, and the entanglement with the cavities A and B is transferred from M to a_2 :

$$\alpha_A |0\rangle_A \otimes \overline{|\psi\rangle}_B \otimes |g\rangle \otimes |0\rangle_M + \beta_A |1\rangle_A \otimes |\psi\rangle_B \otimes |e\rangle \otimes |0\rangle_M. \quad (3.6)$$

At this stage, the state of the cavity M is also factorized and therefore the vector state (3.6) is quantum logically equivalent to that of Eq. (3.3). In practice, the apparatus described here is essentially an *atomic mirror*, which permits us to *reflect back* the atomic state. Finally, let us observe that a_2 has to cross cavity B without interacting with it, before it can reach the cavity A . This result is achieved simply by switching off the classical source S_B ; the adiabatic regime and the

off-resonance condition prevents that, apart from the dynamical phase factors, the state could change during the transit of a_2 within B . The action of the CNOT gate has been explicitly described for the factorized state just to simplify the presentation. It is clear that all the steps can be repeated for a generic entangled state of the two cavities.

Assuming the optimal values for the system parameters written above, we have solved numerically the time evolution of the total system. We describe the resulting effective CNOT gate in the form of a matrix written in the basis of the Fock states of the two cavities, $\{|0,0\rangle; |0,1\rangle; |1,0\rangle; |1,1\rangle\}$ where $|n,m\rangle = |n\rangle_A \otimes |m\rangle_B$. The matrix has been ‘‘cleaned up’’ of the spurious phase factors that may appear during the evolution, and which, using the phase of the classical field S_B and also appropriate Stark shift electrical fields, can always be suitably adjusted. Within a 0.1% error, the optimized CNOT matrix has the form

$$\begin{pmatrix} 0 & e^{-i\lambda} & 0 & 0 \\ e^{i\lambda} & 0 & 0 & 0 \\ 0 & 0 & e^{i\lambda} & 0 \\ 0 & 0 & 0 & e^{-i\lambda} \end{pmatrix}, \quad (3.7)$$

where the nontrivial phase $\lambda = 0.07$. The overall transformation takes place in a time of the order of 1 ms, which has to be compared with the typical decoherence time scales, that is, the atomic radiative lifetimes and the cavity relaxation times. For circular Rydberg atoms with $n \approx 50$, the atomic radiative lifetime is of the order of 30 ms and therefore it does not represent a serious problem. The cavity damping times currently realized for microwaves have instead the same order of magnitude (some ms). However, relaxation times of the order of 10 ms will hopefully be achieved in the near future, and in this case, one would have a perfectly working CNOT gate between two cavities. It is clear therefore that, for the present implementation of quantum information processing, the main source of decoherence in the microwave domain is just the cavity leakage. If optical cavities are instead considered, atomic spontaneous emission may also represent an important source of decoherence.

The matrix of Eq. (3.7) is not a pure CNOTINV gate, even if it is still a universal two-qubit gate [20]; in particular it can be transformed into a standard CNOT gate by adding a single-qubit operation on B , similar to those we shall present in Sec. IV. Moreover, it is also possible to implement the CNOT($A \rightarrow B$) gate (i.e., the one in which the vector component $|1\rangle_A$ causes the NOT transformation on B) simply preparing the first atom entering the apparatus in $|e\rangle$ rather than in $|g\rangle$, and then proceeding with the same identical steps of the CNOTINV case.

The above scheme assumes the possibility of injecting in the apparatus atomic pulses with exactly one atom. However, as shown in Ref. [21], a control of the atom number could be achieved by a modification of the Rydberg-atom preparation technique. The idea is to use an ‘‘atom counter’’ before the circular Rydberg-state preparation, so that the preparation of the state $|e\rangle$ (which can have an efficiency near to 100%) is

applied only when one is sure to have exactly one atom. The atom counter is realized by driving a strong transition and measuring the fluorescence, whose intensity will be proportional to the number of atoms. When the beam section contains zero, two, or more atoms, it is discarded: the system then waits for a time of the order of a few μs to 20 μs (depending upon the atomic velocity and the precise length of the atomic-beam section) until a fresh section of the beam comes in the laser beam driving the fluorescence. In this way, instead of preparing a random number at a given time, one thus prepares with a high probability a single Rydberg atom after a random delay. The average delay is minimal when the probability to have exactly one atom is maximized. With Poissonian statistics, the optimal mean number of atoms is 1. The average random delay could be of the order of 25 μs in a realistic experimental condition. This is short enough at the scale of the cavity-field lifetime to play no major role in the proposed scheme.

IV. QUANTUM PHASE GATE

In the preceding section, we have seen how to implement a universal two-qubit gate, the CNOT gate, between two cavity modes, using induced transitions between dressed states. However, it is possible to realize another universal two-qubit gate, the quantum phase gate (QPG) [4,22], between the two cavities, slightly elaborating on the quantum phase gate operating on qubits carried by the Rydberg atom and the two lowest Fock states of a cavity mode, recently demonstrated experimentally [5]. Of course, since both the CNOT and the QPG are universal quantum gates, it is always possible to implement one of them, by simply supplementing the other one with appropriate one-qubit operations. However, the interesting experimental result of Ref. [5] suggests an alternative physical implementation of quantum logic operations between cavity qubits, which does not involve induced transitions between dressed states, and extends the scheme of [5] to a directly scalable model.

The QPG transformation reads

$$|a,b\rangle \rightarrow \exp(i\phi\delta_{a,1}\delta_{b,1})|a,b\rangle, \quad (4.1)$$

where $|a\rangle$ and $|b\rangle$ describe the basis states $|0\rangle$ and $|1\rangle$ of two generic qubits. This means that the QPG leaves the initial state unchanged except when both qubits are in state $|1\rangle$. In Ref. [5], the QPG of Eq. (4.1) did not involve levels g and e , but i and g , where i is a lower circular Rydberg level, which is uncoupled with the high- Q cavity. In this way, the gate of Eq. (4.1) in the case $\phi = \pi$ can be realized by setting the atomic transition $g \rightarrow e$ perfectly at resonance with the relevant cavity mode (by appropriately Stark shifting the atomic levels inside the cavity), and by selecting the atomic velocity so that the atom undergoes a complete 2π Rabi pulse when crossing the cavity. In fact, at resonance, such a pulse transforms the state $|g,1\rangle$ into $e^{i\pi}|g,1\rangle$, while nothing happens if the atoms is in i or the cavity is in the vacuum state. In [5], the possibility of tuning the phase ϕ over a large

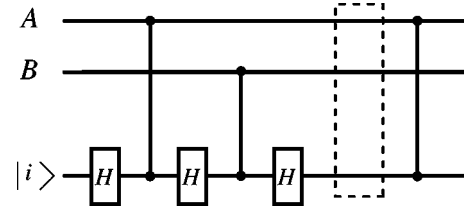


FIG. 5. Logical scheme of the quantum phase gate (QPG) between two cavities. The vertical lines denote the QPG, while H denotes the Hadamard gates (i.e., $\pi/2$ pulses) applied on the atom. The dashed box denotes the ‘‘atomic mirror’’ (see Sec. III).

range, by slightly detuning the cavity mode from the $g \rightarrow e$ transition, has been shown, but we shall not consider this possibility here.

We now show that this atom-cavity QPG can be used to realize a QPG between two cavity modes, by considering an arrangement very similar to that of the CNOT gate shown in Fig. 3. The cavities A and B are again the two qubits, while M is again the auxiliary cavity needed to ‘‘reflect’’ the atom and disentangle it. The two classical sources inside the cavities S_A and S_B are no longer needed, while we consider the possibility of applying Stark shift electric fields inside the cavities, in order to tune the $g \rightarrow e$ transition in and out of resonance from the cavity mode. The scheme of the QPG implementation is shown in Fig. 5 and involves only two atom crossings, as in the CNOT gate of the preceding section, and three $\pi/2$ pulses between the i and g levels (the Hadamard gates H of Fig. 5), which can be realized with resonant classical microwave sources applied between the high- Q cavities.

Let us assume a generic state of the two cavity qubits

$$|\psi\rangle = a_0|00\rangle + a_1|01\rangle + a_2|10\rangle + a_3|11\rangle, \quad (4.2)$$

and that a first atom, initially prepared in state i , is subject to a $\pi/2$ pulse, so to enter cavity A in state $(|i\rangle + |g\rangle)/\sqrt{2}$. The cavity mode is perfectly resonant with the $g \rightarrow e$ transition and the atom velocity is selected so that the atom undergoes a 2π Rabi pulse if it is in state g and the cavity contains one photon (the QPG of Ref. [5]). The resulting state at the exit of cavity A is

$$\frac{|i\rangle \otimes |\psi\rangle}{\sqrt{2}} + \frac{|g\rangle}{\sqrt{2}} \otimes (a_0|00\rangle + a_1|01\rangle - a_2|10\rangle - a_3|11\rangle). \quad (4.3)$$

Then the atom undergoes another resonant $\pi/2$ pulse on the $i \rightarrow g$ transition and the state of the system becomes

$$|i\rangle \otimes (a_0|00\rangle + a_1|01\rangle) + |g\rangle \otimes (a_2|10\rangle + a_3|11\rangle). \quad (4.4)$$

Then the atom crosses cavity B , where it is subjected again to the atom-cavity QPG as in cavity A , so that the state of the system becomes

$$|i\rangle \otimes (a_0|00\rangle + a_1|01\rangle) + |g\rangle \otimes (a_2|10\rangle - a_3|11\rangle). \quad (4.5)$$

At this point, as in the CNOT case of the preceding section, in order to realize the final transformation and disentangle the atom from the cavities, one has to “reflect” it. This is again achieved with the “atomic mirror” scheme, i.e., using the auxiliary cavity M of Fig. 5, which acts as a quantum memory and is able to transfer the entanglement from the first atom to a second atom, which is crossing the apparatus with the same absolute velocity but in the opposite direction [see, for example, Eqs. (3.5) and (3.6)].

The second atom is then subjected to a $\pi/2$ pulse before entering the cavities and the state of Eq. (4.5) becomes

$$\begin{aligned} & \frac{|i\rangle}{\sqrt{2}} \otimes (a_0|00\rangle + a_1|01\rangle + a_2|10\rangle - a_3|11\rangle) \\ & + \frac{|g\rangle}{\sqrt{2}} \otimes (a_0|00\rangle + a_1|01\rangle - a_2|10\rangle + a_3|11\rangle). \end{aligned} \quad (4.6)$$

The last step is the QPG between the atom and cavity A , i.e., the atom has to cross cavity B undisturbed (this is achieved by strongly detuning the $g \rightarrow e$ transition with a Stark shift field) and then has to undergo another full Rabi cycle in cavity A . The final state is

$$\frac{|i\rangle + |g\rangle}{\sqrt{2}} \otimes (a_0|00\rangle + a_1|01\rangle + a_2|10\rangle - a_3|11\rangle), \quad (4.7)$$

which is the desired result, corresponding to a QPG between cavities A and B with conditional phase shift $\phi = \pi$, and with a disentangled atom.

V. ONE-QUBIT OPERATIONS

One-qubit operations are straightforward to implement on qubits represented by two internal atomic states because it amounts to applying suitable Rabi pulses. This task is less trivial for bosonic degrees of freedom such as our cavity modes, because the two lowest Fock states, for example, are coupled to the more excited ones. The most practical solution is to implement one-qubit operations again sending atoms through the cavity. To be more specific, one has to send an atom prepared in the ground state $|g\rangle$ through the cavity, with the classical field S tuned at the frequency corresponding to the transition between the states $|\mathcal{V}_-^{(0)}(t=0)\rangle$ and $|g,0\rangle$. If one sets the time duration and the intensity of the classical source S as in the case of the CNOT(cavity \rightarrow atom), i.e., to realize such a π pulse between the selected levels, one implements a “NOT-phase” gate, which, in the canonical basis $\{|0\rangle, |1\rangle\}$, is described by the following matrix:

$$N(\theta) = \begin{pmatrix} 0 & e^{-i\theta} \\ e^{i\theta} & 0 \end{pmatrix}, \quad (5.1)$$

where θ depends linearly on the phase φ_S of the classical field of Eq. (3.2) and is therefore easily controllable [this scheme is simply a part of the CNOTINV($A \rightarrow B$) gate pre-

sented before]. If on the other hand the atom inside the cavity undergoes a $\pi/2$ instead of a π pulse, one realizes the “Hadamard-phase” gate

$$H(\theta') = \frac{1}{\sqrt{2}} \begin{pmatrix} 1 & e^{-i\theta'} \\ e^{i\theta'} & -1 \end{pmatrix}, \quad (5.2)$$

where θ' also depends linearly on the classical field phase φ_S and is therefore controllable. $N(\theta)$ and $H(\theta')$ can be used to build the more general one-qubit operation and therefore, together with CNOTINV($A \rightarrow B$), form a universal set of gates.

Note that the NOT-phase gate can also be used for an alternative realization of the CNOTINV($A \rightarrow B$) gate between two cavities. In the scheme described in the preceding section, one needs the auxiliary cavity M and the second atom crossing in the opposite direction in order to disentangle the first atom from the cavities. One could simplify this last stage [step (iii) and (iv) of the preceding section] by applying an exact $\pi/2$ pulse when the atom has just left the second cavity and the state of the system is that of Eq. (3.3). The total state becomes

$$\begin{aligned} & \alpha_A |0\rangle_A \otimes \overline{|\psi\rangle}_B \otimes \frac{|g\rangle + |e\rangle}{\sqrt{2}} + \beta_A |1\rangle_A \otimes |\psi\rangle_B \otimes \frac{|g\rangle - |e\rangle}{\sqrt{2}} \\ & = \{ \alpha_A |0\rangle_A \otimes \overline{|\psi\rangle}_B + \beta_A |1\rangle_A \otimes |\psi\rangle_B \} \otimes |g\rangle / \sqrt{2} \\ & + \{ \alpha_A |0\rangle_A \otimes \overline{|\psi\rangle}_B - \beta_A |1\rangle_A \otimes |\psi\rangle_B \} \otimes |e\rangle / \sqrt{2}. \end{aligned} \quad (5.3)$$

If now the atom is detected by a state-sensitive detector and the $|g\rangle$ state is detected, the two cavities are projected on $\alpha_A |0\rangle_A \otimes \overline{|\psi\rangle}_B + \beta_A |1\rangle_A \otimes |\psi\rangle_B$ and one has implemented just the desired CNOTINV gate. On the contrary, if the atom is found in the excited state $|e\rangle$, the state of A and B becomes $\alpha_A |0\rangle_A \otimes \overline{|\psi\rangle}_B - \beta_A |1\rangle_A \otimes |\psi\rangle_B$ and the CNOTINV gate is obtained once that cavity A is subject to a π -phase shift, which can be realized by means of two NOT-phase gates $N(\theta)$, the first with $\theta = \pi/2$ and the second with $\theta = 0$. In this way the atom is disentangled by the measurement. However, the practical application of this scheme is seriously limited by the quantum efficiency of atomic detectors, which is usually far from 100%.

VI. MANY-QUBIT GATES

A. The Toffoli gate

We have shown how to implement a set of universal quantum gates with the proposed cavity QED scheme. Therefore in principle the most general quantum operation involving n qubits can be realized in terms of the one- and two-qubit operations described above. This decomposition, however, implies a degree of network complexity, and a number of resources and steps that is rapidly increasing with the number of qubits n . One of the main advantages of the present proposal is that it is particularly suited for the efficient implementation of many-qubit quantum gates, which,

in many cases, can be realized with the same number of steps as the two-qubit CNOT gate of Sec. III.

A particularly clear example of the possibilities of the proposed scheme is provided by the Toffoli gate [23]

$$|x\rangle_A|y\rangle_B|z\rangle_C \rightarrow |x\rangle_A|y\rangle_B|[z + (x \wedge y)]_{\text{mod}2}\rangle_C, \quad (6.1)$$

in which the target qubit C is controlled by the first two, A and B . The effect of the Toffoli gate on the generic three-qubit state

$$|\Psi_0\rangle = \alpha_1|000\rangle + \alpha_2|001\rangle + \alpha_3|010\rangle + \alpha_4|011\rangle + \alpha_5|100\rangle + \alpha_6|101\rangle + \alpha_7|110\rangle + \alpha_8|111\rangle \quad (6.2)$$

($|n, m, l\rangle = |n\rangle_A \otimes |m\rangle_B \otimes |l\rangle_C$ are the tensor product of the cavity mode Fock states) is to exchange the last two components $|110\rangle$ and $|111\rangle$. The implementation of this gate needs the same arrangement of aligned cavities crossed by Rydberg atoms used for the CNOT gate of Fig. 3, except that now one has *three* cavity qubits (with the corresponding classical sources S_A , S_B , and S_C) instead of two. The auxiliary cavity M is again needed for the atomic mirror scheme used to disentangle the atom. The atom is initially prepared in state $|g\rangle$, and when it is in the first cavity A , it is subject to a π pulse between the dressed state $|\mathcal{V}_+^{(0)}(0)\rangle$ and $|g, 0\rangle$. This pulse creates atom-cavity entanglement and the state of the total system becomes

$$[\alpha_1|000\rangle + \alpha_2|001\rangle + \alpha_3|010\rangle + \alpha_4|011\rangle] \otimes |e\rangle + [\alpha_5|100\rangle + \alpha_6|101\rangle + \alpha_7|110\rangle + \alpha_8|111\rangle] \otimes |g\rangle. \quad (6.3)$$

Then, when the atom reaches the second cavity B , it undergoes another π pulse, at the new frequency ω_2 corresponding to the transition between $|g, 0\rangle$ and $|\mathcal{V}_+^{(2)}(0)\rangle$, so that the transformation

$$|0\rangle_B \otimes |g\rangle \rightarrow |2\rangle_B \otimes |e\rangle \quad (6.4)$$

is realized. This means temporarily leaving the logical subspace, even though this allows us to realize a significant simplification of the scheme. The state after this second step is therefore

$$[\alpha_1|000\rangle + \alpha_2|001\rangle + \alpha_3|010\rangle + \alpha_4|011\rangle + \alpha_5|120\rangle + \alpha_6|121\rangle] \otimes |e\rangle + [\alpha_7|110\rangle + \alpha_8|111\rangle] \otimes |g\rangle. \quad (6.5)$$

When the atom enters in C , the classical field S_C is applied so as to realize the CNOT(atom \rightarrow cavity C) of Sec. III and the state of Eq. (6.5) becomes

$$[\alpha_1|000\rangle + \alpha_2|001\rangle + \alpha_3|010\rangle + \alpha_4|011\rangle + \alpha_5|120\rangle + \alpha_6|121\rangle] \otimes |e\rangle + [\alpha_7|111\rangle + \alpha_8|110\rangle] \otimes |g\rangle. \quad (6.6)$$

At this point one has to disentangle the atom from the three cavities and adjust the state components in which the cavity

C contains two photons. Both problems can be solved by again using the auxiliary cavity M and a second atom crossing the apparatus in the opposite direction as in the ‘‘atomic mirror’’ configuration of Sec. III. The cavity M transfers the entanglement with the cavities from the first to the second atom, which is not subject to any classical pulse in C . Then the second atom enters B , where it undergoes a π pulse at the frequency ω_2 , which simply inverts the transformation of Eq. (6.4) (thanks to the fact that no $|0\rangle_B \otimes |g\rangle$ term is present), correcting in this way the terms of Eq. (6.6) in which the second cavity contains two photons. As a consequence, the state of the atom-cavities system becomes

$$[\alpha_1|000\rangle + \alpha_2|001\rangle + \alpha_3|010\rangle + \alpha_4|011\rangle] \otimes |e\rangle + [\alpha_5|100\rangle + \alpha_6|101\rangle + \alpha_7|111\rangle + \alpha_8|110\rangle] \otimes |g\rangle. \quad (6.7)$$

Finally, the atom enters A , where it is subjected to a π pulse resonant with the transition $|\mathcal{V}_+^{(0)}(0)\rangle \rightarrow |g, 0\rangle$, exchanging $|0\rangle_A \otimes |g\rangle$ with $|0\rangle_A \otimes |e\rangle$, so that the second atom is disentangled from the cavities and one gets the desired generic output of a Toffoli gate, i.e.,

$$[\alpha_1|000\rangle + \alpha_2|001\rangle + \alpha_3|010\rangle + \alpha_4|011\rangle + \alpha_5|100\rangle + \alpha_6|101\rangle + \alpha_7|111\rangle + \alpha_8|110\rangle] \otimes |g\rangle. \quad (6.8)$$

Notice that in this way we have implemented the Toffoli gate with two atoms only, as in the CNOT gate of Sec. III. Moreover, this scheme can be easily extended to the case of $n \geq 4$ cavity qubits, for the implementation of the n -qubit generalization of the Toffoli gate. We need only two atoms crossing the aligned cavities in opposite directions in this more general case. The pulse sequence is similar to that discussed above: both atoms undergo a π pulse resonant with the transition $|\mathcal{V}_+^{(0)}(0)\rangle \rightarrow |g, 0\rangle$ in the first cavity, while in the following $n-2$ cavities they are submitted to a π pulse at the frequency ω_2 . In the last cavity, the target qubit, the first atom experiences a CNOT(atom \rightarrow cavity) while the second atom crosses it undisturbed. In the scheme proposed here, the target qubit is necessarily the last cavity. However, it is always possible to realize the n -qubit generalized Toffoli gate with the target qubit in a generic position of the string of cavities by simply applying a two-qubit operation to the above scheme. In our scheme this means using four atoms at most, and in any case this is much more convenient than realizing this generic n -qubit gate from one- and two-qubit operations.

B. Encoding and decoding in quantum error correction codes

Other examples for which the present cavity QED scheme offers the possibility of an efficient implementation of operations involving many qubits are the encoding and decoding processes used in quantum error correction schemes [24,25]. Errors in quantum information processing are due to the interaction with uncontrolled degrees of freedom (the environment), yielding an entanglement of the quantum state of the register with some environmental states. The main idea of

quantum error correction is to combat “bad” entanglement with “good” entanglement, that is, to protect quantum information by storing it not in a single qubit but in an entangled state of n qubits. This is the encoding process; if the error rate is not too large, it is possible to recover the original quantum information by using a suitable decoding procedure, because the eventual data corruption can be revealed by a measurement on the auxiliary qubits and information can finally be restored with single-qubit operations. The more general one-qubit error (flip error, phase error, or a combination of the two) can always be corrected using a five-qubit encoding and decoding procedure [24,25]. However, if one considers one specific form of error only, three-qubit encoding is sufficient for the implementation of quantum error correction codes. For simplicity, let us consider this latter case.

Let us assume that we want to protect a generic state $\alpha|0\rangle_A + \beta|1\rangle_A$ of the cavity A . For the encoding process, one needs two other ancilla qubits, cavity B and C , and one has to realize the following transformation into a maximally entangled, Greenberger-Horne-Zeilinger state [26] of three cavities:

$$[\alpha|0\rangle_A + \beta|1\rangle_A] \otimes |0\rangle_B \otimes |0\rangle_C \rightarrow \alpha|000\rangle + \beta|111\rangle. \quad (6.9)$$

This encoding process can be realized using a scheme analogous to those discussed above for the CNOT and Toffoli gates. Again, only two atoms are needed, with the second one crossing the aligned cavities in the opposite direction, which serves the purpose of disentangling the first atom, with the help of the auxiliary cavity M in the “atomic mirror” scheme described in Sec. III.

The initial state of the system is

$$[\alpha|0\rangle_A + \beta|1\rangle_A] \otimes |0\rangle_B \otimes |0\rangle_C \otimes |e\rangle \\ \equiv [\alpha|000\rangle + \beta|100\rangle] |e\rangle. \quad (6.10)$$

When the atom enters A it undergoes the CNOT(cavity $A \rightarrow$ atom); when the atom arrives in B , the classical field S_B is switched on in order to realize the CNOT(atom \rightarrow cavity B) transformation (see Sec. III) and the same CNOT(atom \rightarrow cavity C) operation is applied when the atom is in C . One can show that the state of the total system becomes

$$[\alpha|000\rangle|e\rangle + \beta|111\rangle|g\rangle]. \quad (6.11)$$

Except for the entanglement with the atom, the state of A , B , and C is of the desired form, and therefore the situation is analogous to that of the CNOT gate of Sec. III [see Eq. (3.3)]. Atom disentanglement can be obtained by again using the atomic mirror scheme of Sec. III, or eventually, the atomic detection scheme discussed in Sec. IV, which is, however, seriously limited by detector inefficiencies. The logical transformations we have implemented in this section are schematically described in Fig. 6 (the dotted line box represents the atomic mirror).

Decoding is obtained by repeating exactly the same procedure adopted for encoding the state and assuming as an

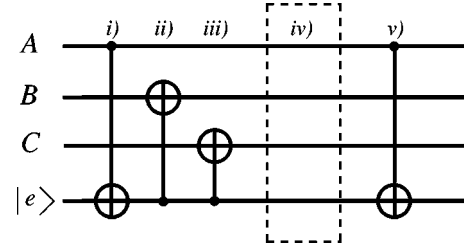


FIG. 6. Logical scheme of the encoding network of Eq. (6.9); qubits B and C are initially prepared in the vacuum state, while A is the qubit storing the initial information. The dashed box $iv)$ represents the atomic mirror described in Sec. III.

initial condition for the qubits set the encoded state (6.9). It is straightforward to check that this amounts to realizing the inverse transformation

$$\alpha|000\rangle + \beta|111\rangle \rightarrow \alpha|000\rangle + \beta|100\rangle \\ = [\alpha|0\rangle_A + \beta|1\rangle_A] \otimes |0\rangle_B \otimes |0\rangle_C. \quad (6.12)$$

It is also easy to see that the encoding scheme described here can be extended for the controlled preparation of maximally entangled states of n cavities. One has to consider n cavities (plus the auxiliary cavity M) and, as in the $n=3$ case, one needs only two atoms crossing the $n+1$ aligned cavities in opposite directions. In analogy with the description above, in the first cavity the two atoms undergo the CNOT(cavity $A \rightarrow$ atom) transformation, while in all the other $n-1$ cavities the first atom goes to a CNOT(atom \rightarrow cavity) gate and the second one crosses them with no classical field applied. In this way, thanks to the disentanglement action of the second atom, the following maximally entangled state of n cavities is prepared:

$$[\alpha|0\rangle_1 + \beta|1\rangle_1] |0\rangle_2 \dots |0\rangle_n \rightarrow \alpha|00\dots 0\rangle + \beta|11\dots 1\rangle. \quad (6.13)$$

VII. CONCLUSIONS

In this paper we have presented a scheme for implementing quantum logic operations within a cavity QED configuration. The quantum register is composed by a series of high- Q cavities and information is encoded in the two lowest cavity Fock states. Both the preparation and the detection of the quantum state of individual qubits, which is an essential ingredient in quantum algorithms, can be easily performed. In particular, the detection of the two Fock states could even be performed in a quantum nondemolition way, as recently demonstrated [13]. Both one- and two-qubit operations can be performed by sending appropriately prepared atoms through the cavities. An important advantage of the scheme is that it is particularly suitable for the direct implementation of some useful many-qubit quantum gates, such as, for example, the Toffoli gate and its n -qubit generalization, or the encoding-decoding network of quantum error correction codes. The scheme could be implemented in a generic cavity QED scheme, even if here we have specialized to the case of microwave cavities and circular Rydberg atoms, for which entanglement manipulation has already been demonstrated

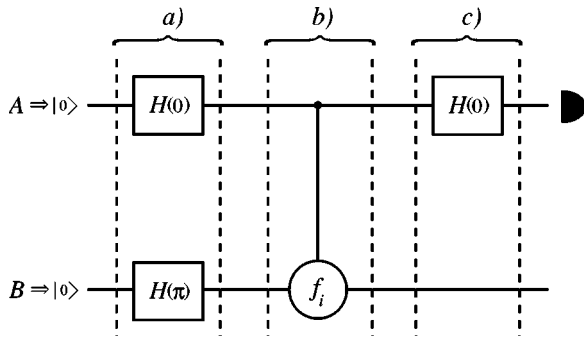


FIG. 7. The Deutsch gate. The box with $H(\theta)$ performs a ‘Hadamard-phase’ transformation on the qubit with phase θ [see Eq. (5.2)].

[5,13]. For example, the same scheme could be adapted to the optical frequency domain, by using high- Q optical cavities, as for example the whispering gallery modes of silica microspheres [27], in which one can have a miniaturization of the scheme and, therefore, a faster gate operation. The scheme proposed here is in principle scalable, even if in practice its scalability will be limited by various factors. In the microwave case one is limited by the spontaneous emission from the circular Rydberg levels (≈ 30 ms) and by the fact that all of the apparatus has to be cooled at cryogenic temperatures to avoid the thermal radiation. In the optical case, cooling is no longer needed and the limitations due to the spontaneous emission could be avoided in principle by using atomic Λ transitions and adiabatic passage through a dark state [28]. However, in the microwave case, the proposed quantum gates could be implemented using available technology, and therefore proof-of-principle demonstrations of quantum computation with, say, ten qubits could be achievable. Instead, even if whispering gallery modes in microspheres with $Q \approx 10^9$ have already been realized [27], en-

tanglement manipulation in this case has not been experimentally demonstrated yet.

Recently, a similar proposal using the two lowest Fock states of a high- Q cavity as a logical qubit has been presented, involving an engineered network of defects in a photonic band-gap material [29]. This proposal is promising with respect to scalability since, using atoms traveling along engineered waveguides in the photonic band-gap material, spontaneous emission could be completely eliminated. However, even if this proposal is promising in terms of the technological realization, in this case, as in the silica microsphere case, entanglement manipulation has not yet been experimentally demonstrated.

From a general point of view, the scheme proposed here is analogous to the linear ion trap scheme, except that now the high- Q cavities play the role of the ions, and the atoms, and not the collective center-of-mass motion, play the role of the quantum bus. At first sight, it may seem unpractical to reverse the role of atoms and photons as we have done here, since the common wisdom is that atoms and ions are suitable for *storing* information while photons are best suited to *transfer* quantum information between different sites. However, the practical implementation of quantum algorithms on linear ion traps is presently limited by the heating of the center-of-mass motion [30]. On the contrary, in the case of photonic qubits discussed here, once the limitations due to the spontaneous emission are eliminated (as in the photonic band-gap case and in the microsphere case with dark-state transitions), the scheme is then only limited by the decoherence due to the finite Q of the cavities, which could reach, however, values of the order of 10^{10} , allowing therefore a sufficient number of gate operations. Moreover, in view of the fact that photons are in any case the best tools for quantum information transport, it may nonetheless be useful to have schemes able to process and temporarily store quantum information using photons.

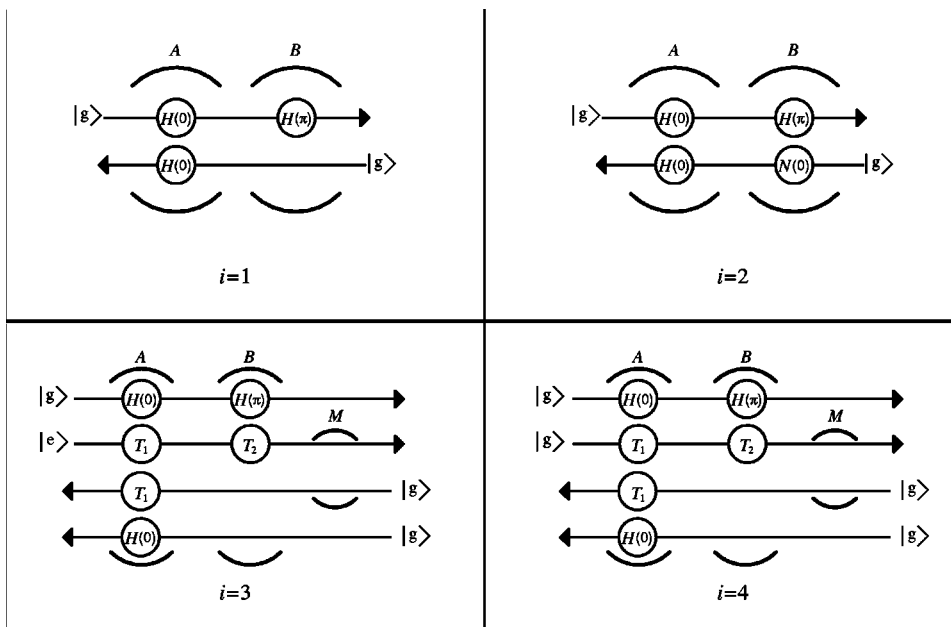


FIG. 8. Physical implementation of the Deutsch gate: $N(\theta)$ and $H(\theta')$ are the one-qubit transformations of Eqs. (5.1) and (5.2); T_1, T_2 are the CNOT(atom \rightarrow cavity) and CNOT(cavity \rightarrow atom), respectively. The index i corresponds to the four different functions $f_i(x)$.

APPENDIX: A REALIZATION OF THE DEUTSCH ALGORITHM

As an example of a simple algorithm that can be implemented with the quantum gates presented before, we consider the Deutsch algorithm [15] in the improved version of Ref. [16]. Consider a generic Boolean function $f(x)$ mapping $\{0,1\}$ into $\{0,1\}$. There are four different possibilities, the two constant functions $f_1(x)=0$, $f_2(x)=1$, and the two *balanced* functions $f_3(x)=x$, $f_4(x)=1-x$. Using classical algorithms, the distinction between these two different classes of functions necessarily requires that *both* values of $f(x)$ have to be evaluated. On the contrary, the Deutsch quantum algorithm solves the problem in just one step. We have to consider the quantum circuit of two cavities in Fig. 7. Initially both cavities are in the vacuum state; then they are submitted to the Hadamard-phase transform of Eq. (5.2), with phases equal to 0 and π , respectively, [step (a) of Fig. 7]. As shown in Sec. IV, this transformation can be implemented with a single atom prepared in the ground state $|g\rangle$ crossing both cavities. At this point the system undergoes the transformation of step (b), namely, the following “ f ” gate:

$$|x\rangle_A |y\rangle_B \rightarrow |x\rangle_A |[y+f_i(x)]_{\text{mod}2}\rangle_B, \quad (\text{A1})$$

where $f_i(x)$, $i=1,2,3,4$ are the four functions defined above, and $[y+f_i(x)]_{\text{mod}2}$ means addition modulo 2. For $i=1$,

this means that nothing happens to the system; on the contrary, for $i=2$ A remains unchanged but the second qubit in cavity B undergoes a NOT transformation. Finally, it is easy to verify that for $i=3$ and for $i=4$ the f gate of Eq. (A1) is equivalent to the CNOT gate and to the CNOTINV gate, respectively. In the preceding sections we have seen how to implement all these transformations. At stage (c) we have then to implement another Hadamard transformation with the zero phase on A and measure the state of this qubit. According to the logical network of Fig. 7, it is possible to show that if the $f_i(x)$ of the f gate is a constant function, then the cavity A must be found in $|0\rangle_A$, otherwise, if $f_i(x)$ is a balanced function, the cavity A will be in $|1\rangle_A$: in this way, one can establish if the function f_i is constant or balanced using a single function evaluation. The physical implementation of the Deutsch problem in terms of the cavities is sketched in Fig. 8. In the case of the constant function it is possible to only use two atoms, because for $i=2$ one atom is needed for the NOT transformation on the cavity B of stage (b) and another atom is needed for the Hadamard transform on the cavity A at step (c). For the balanced functions, the number of atoms is instead equal to four, because, besides the two atoms for the implementation of the Hadamard transformations, one has to use two atoms for the CNOT (if $i=3$) or the CNOTINV (if $i=4$).

-
- [1] C.H. Bennett and D.P. DiVincenzo, *Nature (London)* **404**, 247 (2000).
- [2] J.I. Cirac and P. Zoller, *Phys. Rev. Lett.* **74**, 4091 (1995).
- [3] I.L. Chuang, L.M.K. Vandersypen, X. Zhou, D.W. Leung, and S. Lloyd, *Nature (London)* **393**, 143 (1998); J.A. Jones, M. Mosca, and R.H. Hansen, *ibid.* **393**, 344 (1998).
- [4] Q.A. Turchette, C.J. Hood, W. Lange, H. Mabuchi, and H.J. Kimble, *Phys. Rev. Lett.* **75**, 4710 (1995).
- [5] A. Rauschenbeutel, G. Nogues, S. Osnaghi, P. Bertet, M. Brune, J.M. Raimond, and S. Haroche, *Phys. Rev. Lett.* **83**, 5166 (1999).
- [6] C. Monroe, D.M. Meekhof, B.E. King, W.M. Itano, and D.J. Wineland, *Phys. Rev. Lett.* **75**, 4714 (1995).
- [7] C.A. Sackett, D. Kielpinski, B.E. King, C. Langer, V. Meyer, C.J. Myatt, M. Rowe, Q.A. Turchette, W.M. Itano, D. Wineland, and C. Monroe, *Nature (London)* **404**, 256 (2000).
- [8] S.L. Braunstein *et al.*, *Phys. Rev. Lett.* **83**, 1054 (1999).
- [9] D.P. DiVincenzo, LANL e-print quant-ph/0002077.
- [10] A. Barenco, D. Deutsch, A. Ekert, and R. Jozsa, *Phys. Rev. Lett.* **74**, 4083 (1995).
- [11] T. Sleator and H. Weinfurter, *Phys. Rev. Lett.* **74**, 4087 (1995).
- [12] P. Domokos, J.M. Raimond, M. Brune, and S. Haroche, *Phys. Rev. A* **52**, 3554 (1995).
- [13] G. Nogues, A. Rauschenbeutel, S. Osnaghi, M. Brune, J.M. Raimond, and S. Haroche, *Nature (London)* **400**, 239 (1999).
- [14] V. Giovannetti, P. Tombesi, and D. Vitali, *J. Mod. Opt.* (to be published).
- [15] D. Deutsch, *Proc. R. Soc. London, Ser. A* **400**, 97 (1985).
- [16] R. Cleve, A. Ekert, C. Macchiavello, and M. Mosca, *Proc. R. Soc. London, Ser. A* **454**, 339 (1998).
- [17] S. Haroche and J.M. Raimond, in *Cavity Quantum Electrodynamics*, Special edition of *Adv. At., Mol., Opt. Phys.* **2**, 123 (1994), edited by P. Berman.
- [18] A. Messiah, *Quantum Mechanics* (North Holland, Amsterdam, 1962).
- [19] X. Maitre, E. Hagley, G. Nogues, C. Wunderlich, P. Goy, M. Brune, J.M. Raimond, and S. Haroche, *Phys. Rev. Lett.* **79**, 769 (1997).
- [20] A. Barenco *et al.*, *Phys. Rev. A* **52**, 3457 (1995).
- [21] M. Fortunato, J.M. Raimond, P. Tombesi, and D. Vitali, *Phys. Rev. A* **60**, 1687 (1999).
- [22] S. Lloyd, *Phys. Rev. Lett.* **75**, 346 (1995).
- [23] T. Toffoli, *Lect. Notes in Comp. Science* **84**, 632 (1980).
- [24] R. Laflamme, C. Miquel, J.P. Paz, and W.H. Zurek, *Phys. Rev. Lett.* **77**, 198 (1996).
- [25] E. Knill and R. Laflamme, *Phys. Rev. A* **55**, 900 (1997).
- [26] D.M. Greenberger, M.A. Horne, and A. Zeilinger, *Am. J. Phys.* **58**, 1131 (1990).
- [27] D.S. Weiss, V. Sandoghdar, J. Hare, V. Lefevre-Seguin, J.M. Raimond, and S. Haroche, *Opt. Lett.* **20**, 1835 (1995); M.L. Gorodetsky, A.A. Savchenkov, and V.S. Ilchenko, *ibid.* **21**, 453 (1996); D.W. Vernooy, A. Furusawa, N. Ph. Georgiades, V.S. Ilchenko, and H.J. Kimble, *Phys. Rev. A* **57**, R2293 (1998).

- [28] J.R. Kuklinski, U. Gaubatz, F.T. Hioe, and K. Bergmann, Phys. Rev. A **40**, 6741 (1990); A.S. Parkins, P. Marte, P. Zoller, O. Carnal, and H.J. Kimble, *ibid.* **51**, 1578 (1995).
- [29] N. Vats, T. Rudolph, and S. John, LANL e-print quant-ph/9910046.
- [30] D.J. Wineland, C. Monroe, W.M. Itano, D. Leibfried, B.E. King, and D.M. Meekhof, J. Res. Natl. Inst. Stand. Technol. **103**, 259 (1998).